Article

Severe viral respiratory infections in children with IFIH1 loss-of-function mutations

ASGARI, Samira, *et al*.

Abstract

Viral respiratory infections are usually mild and self-limiting; still they exceptionally result in life-threatening infections in previously healthy children. To investigate a potential genetic cause, we recruited 120 previously healthy children requiring support in intensive care because of a severe illness caused by a respiratory virus. Using exome and transcriptome sequencing, we identified and characterized three rare loss-of-function variants in IFIH1, which encodes an RIG-I-like receptor involved in the sensing of viral RNA. Functional testing of the variants IFIH1 alleles demonstrated that the resulting proteins are unable to induce IFN-β, are intrinsically less stable than wild-type IFIH1, and lack ATPase activity. In vitro assays showed that IFIH1 effectively restricts replication of human respiratory syncytial virus and rhinoviruses. We conclude that IFIH1 deficiency causes a primary immunodeficiency manifested in extreme susceptibility to common respiratory RNA viruses.

Reference

ASGARI, Samira, *et al*. Severe viral respiratory infections in children with IFIH1 loss-of-function mutations. *Proceedings of the National Academy of Sciences*, 2017, vol. 114, no. 31, p. 8342-8347

PMID : 28716935
DOI : 10.1073/pnas.1704259114

Severe viral respiratory infections in children with *IFIH1* loss-of-function mutations

Samira Asgari[a,b], Luregn J. Schlapbach[c,d,e], Stéphanie Anchisi[f], Christian Hammer[a,b], Istvan Bartha[a,b], Thomas Junier[a,b], Geneviève Mottet-Osman[f], Klara M. Posfay-Barbe[g], David Longchamp[h], Martin Stocker[i], Samuel Cordey[j], Laurent Kaiser[j], Thomas Riedel[e], Tony Kenna[k], Deborah Long[c,d], Andreas Schibler[c,d], Amalio Telenti[l], Caroline Tapparel[f], Paul J. McLaren[m,n], Dominique Garcin[f], and Jacques Fellay[a,b,1]

[a]Global Health Institute, School of Life Sciences, École Polytechnique Fédérale de Lausanne, Lausanne, 1015, Switzerland; [b]Swiss Institute of Bioinformatics, Lausanne, 1015, Switzerland; [c]Paediatric Critical Care Research Group, Mater Research Institute, University of Queensland, Brisbane, QLD 4101, Australia; [d]Paediatric Intensive Care Unit, Lady Cilento Children's Hospital, Brisbane, QLD 4101, Australia; [e]Pediatric Intensive Care Unit, Department of Pediatrics, Inselspital, University Children's Hospital and University of Bern, 3010, Switzerland; [f]Department of Microbiology and Molecular Medicine, Faculty of Medicine, University of Geneva, Geneva, 1205, Switzerland; [g]Pediatric Infectious Diseases Unit, Geneva University Hospital, Geneva, 1205, Switzerland; [h]Pediatric Intensive Care Unit, Lausanne University Hospital, Lausanne, 1011, Switzerland; [i]Neonatal and Pediatric Intensive Care Unit, Children's Hospital, Lucerne, 6000, Switzerland; [j]Laboratory of Virology, Division of Infectious Diseases, University of Geneva Medical School, Geneva University Hospitals, Geneva, 1205, Switzerland; [k]Institute for Health and Biomedical Innovation, Translational Research Institute, Queensland University of Technology, Brisbane, QLD 4000, Australia; [l]J. Craig Venter Institute, La Jolla, CA 92037; [m]National Laboratory for HIV Genetics, JC Wilt Infectious Disease Research Center, Public Health Agency of Canada, Winnipeg, MB R3E 0W3, Canada; and [n]Department of Medical Microbiology and Infectious Diseases, University of Manitoba, Winnipeg, MB R3T 2N2, Canada

Edited by Jean-Laurent Casanova, The Rockefeller University, New York, NY, and approved June 27, 2017 (received for review March 14, 2017)

Viral respiratory infections are usually mild and self-limiting; still they exceptionally result in life-threatening infections in previously healthy children. To investigate a potential genetic cause, we recruited 120 previously healthy children requiring support in intensive care because of a severe illness caused by a respiratory virus. Using exome and transcriptome sequencing, we identified and characterized three rare loss-of-function variants in *IFIH1*, which encodes an RIG-I-like receptor involved in the sensing of viral RNA. Functional testing of the variants *IFIH1* alleles demonstrated that the resulting proteins are unable to induce IFN-β, are intrinsically less stable than wild-type IFIH1, and lack ATPase activity. In vitro assays showed that IFIH1 effectively restricts replication of human respiratory syncytial virus and rhinoviruses. We conclude that *IFIH1* deficiency causes a primary immunodeficiency manifested in extreme susceptibility to common respiratory RNA viruses.

respiratory syncytial virus | rhinovirus | *IFIH1* | RIG-I-like receptor family | severe pediatric infectious disease

Viral respiratory tract infections are the most common childhood infections worldwide, with close to 100% of children being infected during the first years of life. Whereas the vast majority of viral respiratory infections are mild and self-limiting, more severe disease leads to the hospitalization of about 3% of individuals in each birth cohort (1). In-hospital mortality rates are limited to <1% with intensive care support; still these infections account for 21% of childhood mortality worldwide (2, 3). The main viral pathogens causing lower respiratory tract infections are human respiratory syncytial virus (RSV), enteroviruses [including human rhinoviruses (HRV)], adenoviruses, human metapneumovirus, coronavirus, influenza, and parainfluenza viruses, with RSV being responsible for the majority of the hospitalized pediatric cases (4, 5).

A number of risk factors including socioeconomic and environmental influences, preterm birth, chronic diseases, and immunosuppression are associated with more severe clinical presentation (6). However, ∼1 out of 1,000 children without any known risk factor will require intensive care support due to life-threatening manifestations of common viral respiratory infections. In the absence of established differences in pathogen virulence, we hypothesized that human genetic variation contributes to unusual susceptibility to severe disease due to common viruses. Supporting evidence is provided by a recent study, which showed that rare variants in *IRF7* resulted in life-threatening influenza in an otherwise healthy child (7).

We combined exome sequencing, transcriptomic analysis, and in vitro functional testing to identify and characterize potentially causal genetic variants in a prospective cohort of previously healthy children requiring intensive care support for common respiratory viral infections. We report the identification of a pathogen-restricted immunodeficiency due to loss-of-function variants in *IFIH1*, which result in defective innate recognition of RNA viruses, preventing the activation of an efficient antiviral IFN response.

Results

Study Participants. We enrolled 120 previously healthy children admitted to pediatric intensive care units (PICUs) with respiratory failure due to a common viral respiratory infection. The most common clinical presentation was bronchiolitis (n = 105, 88%) and the median age was 78 d (interquartile range, IQR: 37–769). RSV was the most common pathogen, identified in 67 (56%) of the cases, followed by HRV in 31 (26%) of the cases (Table 1).

Exome Sequencing and Analysis. DNA samples were sequenced to a mean coverage of 70×, with 96% of exonic bases achieving at least 10× coverage and 78% achieving at least 30× coverage. The final set of variants included 2,793 stop-gained single-nucleotide variants (SNVs), 297 splice-site SNVs, and 951 frame-shift indels. Among these putative loss-of-function variants (LoFs), we searched for variants that were homozygous in at least one study participant, and with a higher minor allele frequency in our cohort than in the genome Aggregation Database (gnomAD) (8) and in an in-house

Significance

Life-threatening susceptibility to common respiratory infections in previously healthy children can be indicative of pathogen-specific primary immunodeficiencies due to rare deleterious variants in key genes and pathways of the immune system. These findings have implications for prevention and treatment of susceptible children.

Author contributions: A.T., D.G., and J.F. designed research; S. Asgari, L.J.S., S. Anchisi, C.H., G.M.-O., K.M.P.-B., D. Longchamp, M.S., S.C., L.K., and T.R. performed research; L.J.S., K.M.P.-B., D. Longchamp, M.S., T.K., D. Long, and A.S. contributed new reagents/analytic tools; S. Asgari, S. Anchisi, C.H., I.B., T.J., G.M.-O., S.C., C.T., and P.J.M. analyzed data; and S. Asgari, L.J.S., S. Anchisi, and J.F. wrote the paper.

The authors declare no conflict of interest.

This article is a PNAS Direct Submission.

Freely available online through the PNAS open access option.

[1]To whom correspondence should be addressed. Email: Jacques.Fellay@epfl.ch.

This article contains supporting information online at www.pnas.org/lookup/suppl/doi:10.1073/pnas.1704259114/-/DCSupplemental.

Table 1. Baseline characteristics of the 120 study participants

Parameter	Variable	Median (IQR) or N (%)
Age, d		78 (37–269)
Weight, kg		5.9 (4.4–9.8)
Country of recruitment	Australia	100 (83%)
	Switzerland	20 (17%)
Ethnicity	Caucasian	90 (78%)
	African	4 (4%)
	Asian	4 (4%)
	Australian aboriginal	6 (5%)
	Pacific Islander	11 (10%)
Sex	Male	70 (58%)
	Female	50 (42%)
Clinical phenotype	Bronchiolitis	105 (88%)
	Pneumonia	8 (7%)
	Laryngotracheobronchitis	5 (4%)
	Reactive airway disease	2 (2%)
Virus identified in respiratory sample	RSV	67 (56%)
	Entero/rhinovirus	31 (26%)
	Adenovirus	17 (14%)
	Human bocavirus	9 (8%)
	Influenza	2 (2%)
	Parainfluenza	6 (5%)
	Human metapneumovirus	3 (2%)
	CoV-HKU1	3 (2%)
	CoV-NL63	1 (1%)
Respiratory support	HFNC	99 (83%)
	CPAP or BiPAP	30 (25%)
	Invasive ventilation	31 (26%)
	HFOV	6 (5%)
Length of PICU stay, d		2.7 (1.6–5.0)
Expected mortality	Pediatric index of mortality 2 (%)	0.02 (0.01–0.7)
Observed mortality	Pediatric index of mortality 2 (%)	No fatal case

CoV-HKU1, coronavirus HkU1; CoV-NL63, coronavirus NL63.

collection of 485 exomes. Six putative LoFs fitting these criteria were identified (*SI Appendix*, Table S3). This set included a variant in the IFN induced with helicase C domain 1 (*IFIH1*) gene, which encodes an RIG-I-like cytoplasmic sensor of long double-stranded RNA (dsRNA) and plays a major role in innate immune recognition of RNA viruses (9).

LoF Variants in IFIH1. In total, eight study participants carried putative LoF variants in *IFIH1* (Table 2). Four study participants carried a rare [gnomAD minor allele frequency (MAF) = 0.64%] splicing variant, rs35732034 (Fig. 1*A*): one in homozygous and three in heterozygous form. We used RNA sequencing to characterize the transcriptomic impact of this variant. We observed that the minor allele T causes skipping of exon 14 (IFIH1-Δ14) (Fig. 1*B*), which results in a frame shift and an early stop codon in exon 15. The resulting protein lacks the final 153 amino acids of wild-type IFIH1, including the C-terminal regulatory domain (CTD), which is essential for binding to viral dsRNA (10) (Fig. 1*C*). Western blot analyses of peripheral blood mononuclear cells from the homozygous patient and her heterozygous parents demonstrated that the IFIH1-Δ14 protein is expressed upon in vitro RSV infection (*SI Appendix*, Fig. S1). We identified two additional rare LoF variants in *IFIH1*, present in heterozygous form in a total of four study participants (Fig. 1*A*): the splicing variant rs35337543 ($n = 3$, gnomAD MAF = 0.67%) and the stop-gained variant rs35744605 ($n = 1$, gnomAD MAF = 0.32%). RNA sequencing showed that the minor allele G at rs35337543 causes skipping of exon 8 (IFIH1-Δ8) (Fig. 1*B*), which removes 39 amino acids at the end of the helicase 1 domain and in the linker part between helicase 1 and helicase 2, but does not result in a frame shift. rs35744605 is a stop-gained SNV in exon 10 that leads to the loss of 399 amino acids from the C-terminal end of IFIH1 (IFIH1-ΔCTD) (Fig. 1*C*).

Description of Study Participants Carrying IFIH1 LoF Variants. A 16-mo-old girl was homozygous for rs35732034. She presented with respiratory failure due to RSV infection requiring invasive ventilation. The disease course was complicated by a pulmonary superinfection with *Staphylococcus aureus*. She had a full recovery and did not develop any other severe infection up to the age of 3. Her phenotype and history was otherwise unremarkable. In particular, she did not develop any complication after live vaccine administration. Full blood count, Ig levels and IgG subclasses, and lymphocyte subclasses were within normal limits. Three infants requiring noninvasive respiratory support for bronchiolitis were heterozygous for rs35732034. One of these had recurrent severe viral lower respiratory tract infections leading to repeated PICU admissions during childhood. Three children were heterozygous for rs35337543 and required noninvasive ventilatory support for RSV bronchiolitis. One infant was heterozygous for rs35744605 and required invasive ventilatory support for HRV-positive bronchiolitis. Parental DNA was available for three of the eight children. Targeted genotyping confirmed that the relevant *IFIH1* variant was present in heterozygous form in one of the parents for two heterozygous individuals, and in both parents for the homozygous patient. Parental medical history was unremarkable in all cases.

Functional Characterization of IFIH1 Variants. To functionally characterize the identified variants, we first measured the ability of wild-type (IFIH1-wt) and mutant IFIH1 isoforms to induce IFN β (IFNβ) in vitro. We transfected plasmids carrying IFIH1-wt,

Table 2. Characteristics of the eight study participants carrying an IFIH1 loss-of-function variant

Patient ID	Zygosity	Sex	Age at admission, d	Ethnicity	Virus	Ventilation required	Clinical presentation	Parental allele	Variant ID	Nucleotide change	Amino acid change	gnomAD AC (#hom), MAF
PRI_022	hom	F	493	White	RSV	I	Bronchiolitis pneumonia	het in both parents	rs35732034	2:163124596 C/T	p.Ile872Ter	1673 (7), 0.006
PRI_050	het	M	34	Aboriginal	HRV	NI	Recurrent bronchiolitis	NA				
PRI_061	het	M	41	White	RSV	NI	Bronchiolitis	het in father				
PRI_122	het	F	48	White	RSV	NI	Bronchiolitis	het in mother				
PRI-063	het	M	22	White	RSV	NI	Bronchiolitis	NA	rs35337543	2:163136505 C/G	p.Leu509_Glu547*del*	1847 (8), 0.006
PRI-065	het	M	38	White	RSV	NI	Bronchiolitis	NA				
PRI-116	het	M	479	White	RSV	NI	Bronchiolitis	NA				
PRI-080	het	M	343	White	HRV	I	Bronchiolitis pneumonia	NA	rs35744605	2:163134090 C/A	p.Glu627Ter	887 (1), 0.003

NA, not available; het, heterozygous; hom, homozygous; I, invasive; NI, noninvasive; AC, allele count.

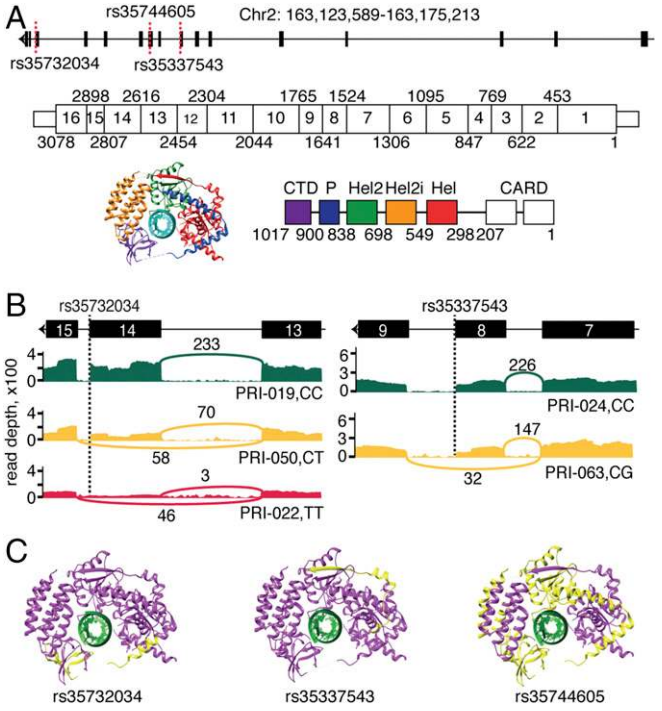

Fig. 1. LoF variants identified in *IFIH1*. Related to *SI Appendix*, Fig. S1. (*A*) Schematic representation of IFIH1 DNA, mRNA, and protein. The identified variants are indicated with dashed red lines. Exon boundaries are marked with nucleotide coordinates. Protein domain boundaries are marked with amino acid coordinates. (*B*) Alternative splicing of IFIH1 associated with rs35732034 and rs35337543 genotypes, as seen in RNA sequencing data. The T allele at rs35732034 leads to skipping of exon 14. The G allele at rs35337543 leads to skipping of exon 8. The Sashimi plots illustrate the genotype-dependent abundance of splice junctions. The number of observed reads spanning the respective splice junctions is indicated on the Bezier curves, which connect exons. (*C*) Schematic 3D representation of IFIH1 (Protein Data Bank ID code: 4GL2, image produced using UCSC Chimera). The parts of the protein that are predicted to be missing due to rs35732034, rs35744605 and rs35337543 variants are indicated in yellow. Hel, helicase domain; P, pincer.

IFIH1-Δ8, IFIH1-Δ14, and IFIH1-ΔCTD into 293T cells. Overexpression of IFIH1-wt, but not of any of the mutant IFIH1 isoforms, led to IFNβ induction. Cotransfection of IFIH1-wt with each of the mutant IFIH1 isoforms showed interference with IFIH1-wt-induced IFNβ production ($P < 0.05$, Fig. 2*A*). We then tested the ATPase activity of recombinant IFIH1-wt and mutant IFIH1 isoforms. IFIH1-wt was able to hydrolyze ATP and showed a typical dsRNA-dependent increase in enzymatic activity, whereas the mutant isoforms had no detectable ATPase activity, even upon stimulation with polyinosinic:polycytidylic acid (polyI:C), a synthetic analog of dsRNA (Fig. 2*B*). Furthermore, all mutant isoforms decreased IFIH1-wt ATPase activity in a dose-dependent manner, an interference that was specific to mutant IFIH1 isoforms, as demonstrated by the absence of any effect of BSA on IFIH1-wt ATPase activity ($P < 0.05$, Fig. 2*C* and *SI Appendix*, Fig. S2 *A* and *B*). Finally, we checked the stability of the various IFIH1 protein isoforms by performing pulse-chase experiments in transfected 293T cells. The three mutant isoforms were less stable than IFIH1-wt (Fig. 2*D*) and had a negative impact on the stability of the wild-type isoform when cotransfected (Fig. 2*E*). Jointly, these experiments demonstrate that the three putative LoF variants identified in our study population lead to severe disruption of IFIH1 signaling function, enzymatic activity, and protein stability in vitro. In addition, the observations that the mutant IFIH1 isoforms interfere with the wild-type protein in terms of IFNβ induction, and enzymatic activity and protein stability suggest a dominant negative role for heterozygous LoF variants in *IFIH1*.

Role of IFIH1 in RSV and HRV Replication. Viral testing of respiratory samples showed that six of the patients harboring *IFIH1* LoF alleles were infected with RSV and two with HRV. To study the effect of IFIH1 on RSV and HRV replication, we used Huh7.5 cells, which lack endogenous expression of IFIH1 and express a mutated, inactive form of RIG-I, and thus are completely unreactive to the RNA pathogen-associated molecular patterns that normally activate these pathways (11). The cells were transduced with an IFIH1-wt-expressing lentiviral vector, which made them highly responsive to polyI:C stimulation (*SI Appendix*, Fig. S3*A*) without causing any nonspecific or constitutive activation of the IFN system (*SI Appendix*, Fig. S3*B*). We observed a much higher level of viral replication in native than in IFIH1-wt-transduced Huh7.5 cells upon infection with HRV-B14, HRV-

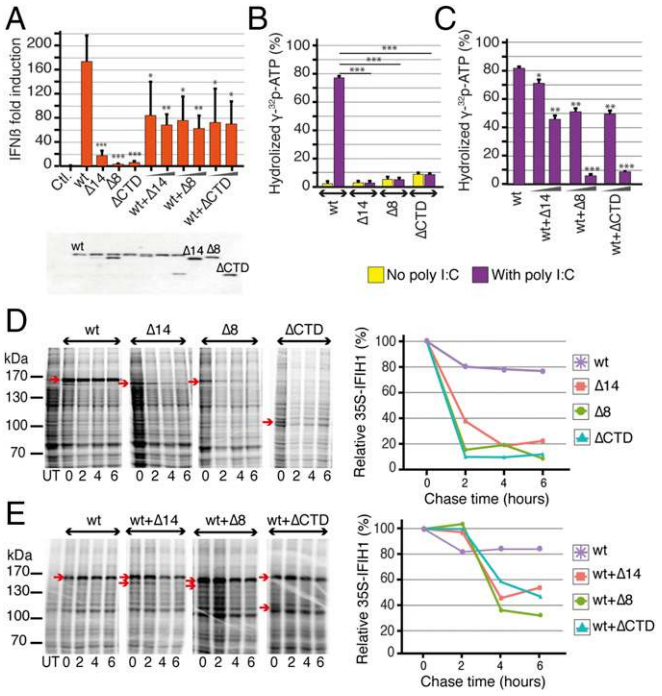

Fig. 2. Functional characterization of the *IFIH1* variants. Related to *SI Appendix*, Fig. S2. (*A*) Transfection with IFIH1-wt plasmid (20 ng) results in strong IFNβ induction in 293T cells, whereas transfection of plasmids harboring any of the *IFIH1* variants cannot induce IFNβ (240 ng, $n = 4$). Cotransfection experiments demonstrate an interference of the mutant plasmids with IFIH1-wt on IFNβ induction (20-ng wt plasmid, 20- and 120-ng mutant plasmids, $n = 4$). Expression levels of the IFIH1 isoforms are shown under the plot in the Western blot gel. $^*P < 0.05$, $^{**}P < 0.01$, $^{***}P < 0.001$. (*B*) RNA-induced ATPase activity of purified IFIH1-wt protein and alternate IFIH1 isoforms; IFIH1-wt can hydrolyze ATP in the presence of polyI:C, whereas IFIH1-Δ14, IFIH1-Δ8, and IFIH1-ΔCTD lack ATPase activity, with (purple) or without (yellow) polyI:C stimulation. (*C*) ATPase activity of IFIH1-wt is reduced upon coincubation with the alternate isoforms in a dose-dependent manner (300-ng wt protein, 300- or 600-ng of each alternate isoform, 10-ng polyI:C, $n = 2$). $^*P < 0.05$, $^{**}P < 0.01$, $^{***}P < 0.001$. (*D* and *E*) Protein stability followed by pulse chase in 293T cells expressing IFIH1-wt, IFIH1-Δ14, IFIH1-Δ8, or IFIH1-ΔCTD. Each protein is marked on the gel by an arrow, and relative amounts of proteins are shown in the graphs. IFIH1-wt is more stable than the alternate IFIH1 isoforms, and the stability of IFIH1-wt is reduced upon coexpression with any of the alternate isoforms. Molecular mass markers are shown on the left of each gel (kilodaltons) and the bands corresponding to IFIH1-wt, IFIH1-Δ14, IFIH1-Δ8, or IFIH1-ΔCTD are indicated using a red arrow (2-μg plasmid expressing wt protein, 2 μg of each mutant plasmid, $n = 1$). Data are represented as mean ± SD; polyI:C, polyinosinic:polycytidylic acid.

A16, and RSV (Fig. 3 *A–D*). Furthermore, RSV replication level was higher in cells transduced with the mutant forms of IFIH1 than in IFIH1-wt-transduced cells ($P < 0.05$, *SI Appendix*, Fig. S4 *A* and *B*). The role of IFIH1 in HRV restriction was further demonstrated by ^{35}S labeling of infected cells, which showed a stronger shutoff of cellular protein synthesis in native than in IFIH1-transduced Huh7.5 cells, due to higher replication of the virus in the absence of IFIH1 (Fig. 3*E*). We also measured RSV replication in mouse embryonic fibroblasts (MEFs), *ifih1*$(^{+/+})$, and in IFIH1-knockout MEFs, *ifih1*$(^{-/-})$, and obtained similar results (Fig. 3 *F–H*). Together, these results affirm the central role of IFIH1 in innate immune recognition of RSV and HRV (12, 13). Therefore, LoF variants in *IFIH1* can be reasonably expected to increase susceptibility to these viruses.

Discussion

We hypothesized that extreme susceptibility to common viral respiratory infection in previously healthy children—a rare, potentially lethal phenotype—could reflect an underlying primary immunodeficiency. Using an unbiased exomewide approach in a prospective cohort of carefully selected individuals requiring intensive care support, we identified a rare monogenic defect predisposing to severe clinical presentations of RSV and HRV infections.

Three deleterious variants were observed in *IFIH1*, which encodes a cytoplasmic receptor critical for viral RNA sensing. It has been shown previously that IFIH1, alone or in combination with RIG-I, recognizes and limits the replication of many RNA viruses including: positive single-stranded RNA (ssRNA) viruses like picornaviruses (14–16), negative ssRNA viruses like paramyxoviruses (17–19), and dsRNA viruses like reoviruses (20).

IFIH1 recognizes viral RNA via interaction of its CTD and helicase domains with long dsRNA molecules. This is an ATP-dependent reaction that leads to polymerization of IFIH1 molecules into a filament and assembly of IFIH1 caspase activation recruitment domains (CARDs) (21, 22). This in turn initiates a signaling cascade that results in type 1 IFN production and activation of antiviral genes (23). Our transfection and transduction analyses show that this process is disrupted in the presence of any of the *IFIH1* rare variants found in our study population. Our exome and RNA sequencing data predict that the loss of IFIH1 function is due to loss of the CTD (rs35732034 and rs35744605) or to partial loss of the helicase domain (rs35337543).

We observed interference between IFIH1-wt and the three mutant proteins in terms of stability, ATPase activity, and capacity to induce IFNβ production, suggesting a dominant negative effect, which provides a rationale for the unusual susceptibility to respiratory viruses observed in heterozygous individuals. The exact interfering mechanism is not known but could involve physical interaction between IFIH1-wt and mutant proteins, preventing the formation of normal, multimeric IFIH1 filaments.

While the revised version of this paper was under review, an independent study showed an association between IFIH1 deficiency and life-threatening infections with HRV and other respiratory viruses in a child carrying another homozygous missense *IFIH1* variant (24). This observation further supports a causal role for IFIH1 deficiency in extreme susceptibility to common respiratory viruses.

The three IFIH1 variants described in this study have allele frequencies of 0.32–0.67% in gnomAD. The cumulative frequency of all putative LoF alleles is 1.89% in the same database, which is significantly less than the 3.75% cumulative frequency observed in our study population ($P = 0.037$, Fisher's exact test). Nevertheless, the presence of alleles of potentially devastating consequences at such frequency in the general population is intriguing, as they are expected to be removed by purifying selection. Two nonexclusive mechanisms can explain this observation: balancing selection and incomplete penetrance. We here show that some *IFIH1* alleles increase susceptibility to viral respiratory infections, but the same LoF variants are known to be protective against type 1 diabetes and other autoimmune diseases (25–30), strongly suggesting a role for balancing selection in their maintenance. In a comparable example, rare nonsynonymous variants in *TYK2*, a known primary immunodeficiency gene, were shown to be protective against rheumatoid arthritis (31). Incomplete penetrance, on the other hand, could be due to modulating effects of environmental or genetic factors, like compensatory mutations, or to functional redundancy in innate immune response to RNA viruses (32, 33). This hypothesis is in line with several recent publications (34–37), which suggest that incomplete penetrance and genetic heterogeneity are likely to be the rule rather than the exception in severe clinical presentations of infectious diseases.

On top of their associations with autoimmunity, more common *IFIH1* variants have also been associated with hepatitis C virus clearance (38). Additionally, rare gain-of-function mutations in *IFIH1* dramatically up-regulate type I IFN production, resulting in Aicardi–Goutières syndrome or Singleton–Merten syndrome (39–41). At the functional level, Gorman et al. recently studied the effects on viral sensing and autoimmune pathogenesis of rs1990760, a missense *IFIH1* variant that is associated with multiple autoimmune diseases (30). They showed that the allele providing better defense against viral infection also bolsters autoimmune responses against self-RNA (42). Together, these results underscore the pivotal role of innate immune recognition and activation in the intricate balance between host defense, inflammation, and autoimmunity.

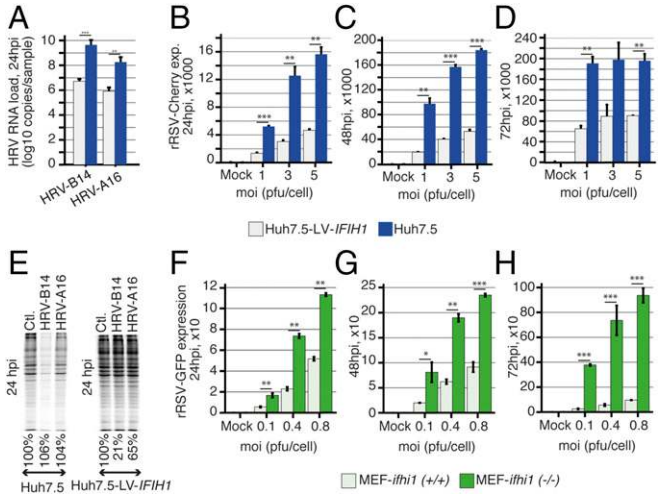

Fig. 3. IFIH1 restricts HRV and RSV replication. Related to *SI Appendix*, Figs. S3 and S4. (*A*) Real-time PCR of HRV-B14 and HRV-A16 RNA in Huh7.5 and Huh7.5 cells transduced with a lentiviral vector expressing IFIH1 (Huh7.5-LV-*IFIH1*). HRV-B14 and HRV-A16 replicate more efficiently in the absence of IFIH1 at 24 h postinfection (hpi) ($n = 5$ for HRV-B14 and $n = 2$ for HRV-B16). $^{*}P < 0.05$, $^{**}P < 0.01$, $^{***}P < 0.001$. (*B–D*) FACS analyses of mCherry expressing recombinant RSV (rRSV-Cherry) in Huh7.5 and Huh7.5-LV-*IFIH1* transduced cells at 24, 48, and 72 hpi show that RSV replicates more efficiently in the absence of IFIH1 ($n = 2$). (*E*) Cellular proteins labeled with ^{35}S at 24 hpi with both HRV-B14, HRV-A16 showing a much stronger shutoff of cellular protein synthesis in Huh7.5 cells than in Huh7.5-LV-*IFIH1* transduced cells, due to higher viral replication. (*F–H*) FACS analyses of GFP expressing recombinant RSV (rRSV-GFP) in *ifih1* knockout MEFs [MEF-*ifih1*$(^{-/-})$] and *ifih1* knockout MEFs transduced with a lentiviral vector expressing IFIH1 (MEF-LV-*IFIH1*). RSV replicates more efficiently in the absence of IFIH1 at 24, 48, and 72 hpi ($n = 2$). $^{*}P < 0.05$, $^{**}P < 0.01$, $^{***}P < 0.001$. Data are represented as mean ± SD. GFP, green florescent protein; MEF, mouse embryonic fibroblast; moi, multiplicity of infection; pfu, plaque-forming unit.

GENETICS

Our study demonstrates the power of using an unbiased, exome sequencing approach to variant discovery in prospective cohorts of extreme infectious disease phenotypes. Nevertheless, LoF variants in *IFIH1* were only found in a minority (n = 8, 6.2%) of the 120 children enrolled in our study, suggesting that other genetic or nongenetic risk factors remain to be discovered. Larger sample sizes will be required to delineate the relevance of other rare potentially causal alleles. Whole genome sequencing will also be needed to obtain a more complete coverage of exonic regions (43), and to explore noncoding and large-scale structural variation.

RSV and rhinovirus infections are the two most common viral respiratory infections in children. The elucidation of the human genetic basis of extreme susceptibility to these viruses provides insight into pathogenesis and innate immune response. An immediate practical implication is the possibility to develop diagnostic assays to identify susceptible individuals who could benefit from specific preventive and interventional measures. By highlighting the genes and pathways that play an essential role in host–pathogen interaction, genetic discovery in individuals with extreme phenotypes also provides the opportunity to design new therapeutic strategies that could be useful for the vast majority of patients with milder clinical presentation.

Materials and Methods

Between December 2010 and October 2013, we prospectively enrolled previously healthy children below 4 y of age suffering from severe lower respiratory tract infection and requiring invasive or noninvasive respiratory support in five specialized PICUs from Australia and Switzerland. The study was approved by the respective institutional Human Research Ethics Committees. Written informed consent was obtained from parents or legal guardians.

Exclusion criteria were the presence of any significant underlying disease or comorbidity, including prematurity, congenital cardiac disease, chronic lung disease, sickle cell disease, hepatic, renal, or neurologic chronic conditions, solid and hematological malignancies, and known primary immunodeficiency. Respiratory support was defined as noninvasive ventilation including high-flow nasal cannulae (HFNC) and continuous or bilevel positive airway pressure (CPAP and BiPAP), or invasive ventilation including conventional and high-frequency oscillation ventilation (HFOV). The following demographic and clinical information was collected: age, gender, weight, ethnicity, type of ventilation, length of ventilation in days, clinical outcome, microbiological diagnostic procedures and results including rapid antigenic test for RSV and influenza, respiratory virus PCR panel, and viral cultures. For each study participant, we obtained a nasopharyngeal aspirate or endotracheal tube aspirate, 1 mL EDTA blood in vacutainer tubes, and 2.5 mL blood in PAXgene blood RNA tubes. Samples were immediately frozen at −70 °C until shipment, and then analyzed in batch.

We generated high-coverage exome sequencing data for all study participants (*SI Appendix*, Table S1). We then used a combination of three variant calling methods (GATK, Platypus, and SAMtools) and only kept SNVs and small insertion and deletions (*SI Appendix*, Table S2). Assuming that causal genetic variants are likely to be highly deleterious, we focused on rare gene knockout events, defined as homozygous, putative LoF variants (stop-gained and splice-site SNVs, frame-shift indels) with an MAF of <1% in the ExAC (*SI Appendix*, Table S3). We performed RNA sequencing to assess the transcriptomic impact of candidate DNA variants, and characterized the infecting viruses using multiplex PCR assays. We then used in vitro functional testing to demonstrate the biological relevance of candidate variants and tested in vivo expression of the affected protein (*SI Appendix*).

ACKNOWLEDGMENTS. We express our sincere appreciation to all study participants and their families for their participation and support. We thank Deon Venter and Marc Vipond, Mater Pathology, Mater Health Services, Brisbane, as well as Patricia Keith, Institute for Health and Biomedical Innovation, Queensland University of Technology, Brisbane, Australia, for their help in sample processing and sampling logistics; Mark Peeples (Columbus, OH) for sharing rRSV-GFP, and Jean-François Eléouët (Institut National de la Recherche Agronomique, Jouy-en-Josas, France) for sharing rRSV- mCherry. mCherry. This study was funded by Swiss National Science Foundation Grants PP00P3_133703 and PP00P3_157529 (to J.F.).

1. Meissner HC (2016) Viral bronchiolitis in children. *N Engl J Med* 374:62–72.
2. Nair H, et al.; Severe Acute Lower Respiratory Infections Working Group (2013) Global and regional burden of hospital admissions for severe acute lower respiratory infections in young children in 2010: A systematic analysis. *Lancet* 381:1380–1390.
3. Liu L, et al. (2015) Global, regional, and national causes of child mortality in 2000-13, with projections to inform post-2015 priorities: An updated systematic analysis. *Lancet* 385:430–440.
4. Jain S, et al.; CDC EPIC Study Team (2015) Community-acquired pneumonia requiring hospitalization among U.S. children. *N Engl J Med* 372:835–845.
5. Debiaggi M, Canducci F, Ceresola ER, Clementi M (2012) The role of infections and coinfections with newly identified and emerging respiratory viruses in children. *Virol J* 9:247.
6. Rodríguez DA, et al. (2014) Predictors of severity and mortality in children hospitalized with respiratory syncytial virus infection in a tropical region. *Pediatr Pulmonol* 49:269–276.
7. Ciancanelli MJ, et al. (2015) Infectious disease. Life-threatening influenza and impaired interferon amplification in human IRF7 deficiency. *Science* 348:448–453.
8. Lek M, et al.; Exome Aggregation Consortium (2016) Analysis of protein-coding genetic variation in 60,706 humans. *Nature* 536:285–291.
9. Kato H, et al. (2006) Differential roles of MDA5 and RIG-I helicases in the recognition of RNA viruses. *Nature* 441:101–105.
10. Takahasi K, et al. (2009) Solution structures of cytosolic RNA sensor MDA5 and LGP2 C-terminal domains: Identification of the RNA recognition loop in RIG-I-like receptors. *J Biol Chem* 284:17465–17474.
11. Zhong J, et al. (2005) Robust hepatitis C virus infection in vitro. *Proc Natl Acad Sci USA* 102:9294–9299.
12. Feng Q, Langereis MA, van Kuppeveld FJ (2014) Induction and suppression of innate antiviral responses by picornaviruses. *Cytokine Growth Factor Rev* 25:577–585.
13. Grandvaux N, et al. (2014) Sustained activation of interferon regulatory factor 3 during infection by paramyxoviruses requires MDA5. *J Innate Immun* 6:650–662.
14. Gitlin L, et al. (2006) Essential role of mda-5 in type I IFN responses to polyriboinosinic:polyribocytidylic acid and encephalomyocarditis picornavirus. *Proc Natl Acad Sci USA* 103:8459–8464.
15. Barral PM, et al. (2007) MDA-5 is cleaved in poliovirus-infected cells. *J Virol* 81:3677–3684.
16. Slater L, et al. (2010) Co-ordinated role of TLR3, RIG-I and MDA5 in the innate response to rhinovirus in bronchial epithelium. *PLoS Pathog* 6:e1001178.
17. Gitlin L, et al. (2010) Melanoma differentiation-associated gene 5 (MDA5) is involved in the innate immune response to Paramyxoviridae infection in vivo. *PLoS Pathog* 6:e1000734.
18. Shingai M, et al. (2007) Differential type I IFN-inducing abilities of wild-type versus vaccine strains of measles virus. *J Immunol* 179:6123–6133.
19. Baños-Lara Mdel R, Ghosh A, Guerrero-Plata A (2013) Critical role of MDA5 in the interferon response induced by human metapneumovirus infection in dendritic cells and in vivo. *J Virol* 87:1242–1251.
20. Loo Y-MM, et al. (2008) Distinct RIG-I and MDA5 signaling by RNA viruses in innate immunity. *J Virol* 82:335–345.
21. Berke IC, Yu X, Modis Y, Egelman EH (2012) MDA5 assembles into a polar helical filament on dsRNA. *Proc Natl Acad Sci USA* 109:18437–18441.
22. Rawling DC, Pyle AM (2014) Parts, assembly and operation of the RIG-I family of motors. *Curr Opin Struct Biol* 25:25–33.
23. Loo Y-MM, Gale M, Jr (2011) Immune signaling by RIG-I-like receptors. *Immunity* 34:680–692.
24. Lamborn IT, et al. (2017) Recurrent rhinovirus infections in a child with inherited MDA5 deficiency. *J Exp Med* 214:1949–1972.
25. Nejentsev S, Walker N, Riches D, Egholm M, Todd JA (2009) Rare variants of IFIH1, a gene implicated in antiviral responses, protect against type 1 diabetes. *Science* 324:387–389.
26. Chistiakov DA, Voronova NV, Savost'Anov KV, Turakulov RI (2010) Loss-of-function mutations E6 27X and I923V of IFIH1 are associated with lower poly(I:C)-induced interferon-β production in peripheral blood mononuclear cells of type 1 diabetes patients. *Hum Immunol* 71:1128–1134.
27. Smyth DJ, et al. (2006) A genome-wide association study of nonsynonymous SNPs identifies a type 1 diabetes locus in the interferon-induced helicase (IFIH1) region. *Nat Genet* 38:617–619.
28. Yang H, et al. (2012) IFIH1 gene polymorphisms in type 1 diabetes: Genetic association analysis and genotype-phenotype correlation in Chinese Han population. *Autoimmunity* 45:226–232.
29. Cen H, et al. (2013) Association of IFIH1 rs1990760 polymorphism with susceptibility to autoimmune diseases: a meta-analysis. *Autoimmunity* 46:455–462.
30. Chistiakov DA (2010) Interferon induced with helicase C domain 1 (IFIH1) and virus-induced autoimmunity: A review. *Viral Immunol* 23:3–15.
31. Diogo D, et al. (2015) TYK2 protein-coding variants protect against rheumatoid arthritis and autoimmunity, with no evidence of major pleiotropic effects on non-autoimmune complex traits. *PLoS One* 10:e0122271.
32. Jensen S, Thomsen AR (2012) Sensing of RNA viruses: A review of innate immune receptors involved in recognizing RNA virus invasion. *J Virol* 86:2900–2910.
33. Xu L, et al. (2016) Loss of RIG-I leads to a functional replacement with MDA5 in the Chinese tree shrew. *Proc Natl Acad Sci USA* 113:10950–10955.
34. Kong X-FF, et al. (2013) Haploinsufficiency at the human IFNGR2 locus contributes to mycobacterial disease. *Hum Mol Genet* 22:769–781.
35. Sancho-Shimizu V, et al. (2011) Herpes simplex encephalitis in children with autosomal recessive and dominant TRIF deficiency. *J Clin Invest* 121:4889–4902.

36. Lim HK, et al. (2014) TLR3 deficiency in herpes simplex encephalitis: High allelic heterogeneity and recurrence risk. *Neurology* 83:1888–1897.
37. Conley ME, Casanova J-LL (2014) Discovery of single-gene inborn errors of immunity by next generation sequencing. *Curr Opin Immunol* 30:17–23.
38. Hoffmann FS, et al. (2015) Polymorphisms in melanoma differentiation-associated gene 5 link protein function to clearance of hepatitis C virus. *Hepatology* 61: 460–470.
39. Rice GI, et al. (2014) Gain-of-function mutations in IFIH1 cause a spectrum of human disease phenotypes associated with upregulated type I interferon signaling. *Nat Genet* 46:503–509.
40. Oda H, et al. (2014) Aicardi-Goutières syndrome is caused by IFIH1 mutations. *Am J Hum Genet* 95:121–125.
41. Rutsch F, et al. (2015) A specific IFIH1 gain-of-function mutation causes Singleton-Merten syndrome. *Am J Hum Genet* 96:275–282.
42. Gorman JA, et al. (2017) The A946T variant of the RNA sensor IFIH1 mediates an interferon program that limits viral infection but increases the risk for autoimmunity. *Nat Immunol* 18:744–752.
43. Gilissen C, et al. (2014) Genome sequencing identifies major causes of severe intellectual disability. *Nature* 511:344–347.

Supplementary information

Supplement to:

Severe viral respiratory infections in children with *IFIH1* loss-of-function mutations

S. Asgari, L. J. Schlapbach, S. Anchisi, C. Hammer, I. Bartha, T. Junier, G. Mottet-Osman, K. Posfay Barbe, D. Longchamp, M. Stocker, S. Cordey, L. Kaiser, T. Riedel, T. Kenna, D. Long, A. Schibler, A. Telenti, C. Tapparel, P. J. McLaren, D. Garcin, J. Fellay

Table S1. Summary metrics of short-read alignment. Related to experimental procedure. PF, pass filter; SD, standard deviation.

	PF unique reads (%)	PF unique reads aligned (%)	Off-bait (%)	Mean bait coverage (%)	At least 2X coverage (%)	At least 30X coverage (%)
Average	0.93	0.96	0.22	69.99	0.99	0.78
SD	0.07	0.04	0.03	15.29	0.01	0.08
Median	0.96	0.97	0.23	68.04	0.99	0.79

Table S2. Summary metrics for variant calling. Related to experimental procedure. Three different variant calling methods were used and the variants in the intersection used for downstream analysis.

Variant caller	GATK	Platypus	SAMtools	Intersection
Total variants (%novel)	287681 (16.74%)	271978 (17.72%)	317820 (18.90%)	242954 (14.14%)
SNV (%novel)	263507 (14.04%)	258548 (16.34%)	296161 (16.63%)	232591 (13.25%)
Indel (%novel)	24174 (46.23%)	13430 (44.34%)	21659 (49.89%)	10363 (34.12%)
FRAME-SHIFT	1644	1333	1415	951
STOP-GAINED	880	942	1082	793
STOP-LOST	89	85	99	76
START-LOST	126	128	144	112
SPLICE-SITE	377	353	446	297
MISSENSE	64057	66559	74945	59144
INFRAME	1854	1102	1811	867
SYNONYMOUS	55698	56964	62381	52261
UTR	23478	16320	19780	14434
LoF (%novel)	2635 (49.44%)	2419 (49.89%)	2710 (46.60%)	1878 (41.64%)
SNP-LoF (%novel)	1116 (30.73%)	1219 (34.12%)	1371 (32.31%)	1023 (30.00%)
Indel-LoF (%novel)	1519 (63.19%)	1200 (65.91%)	1339 (61.23%)	855 (55.55%)

Table S3. Homozygous loss-of-function variants observed in the study population.

Chr, chromosome; MAF, minor allele frequency; NA, not available.

Chr	Position	SNP ID	Gene	Predicted effect	MAF (%) gnomAD	MAF (%) this study
1	26301080	rs375730731	PAFAH2	STOP-GAINED	<0.01	2.08
2	163124596	rs35732034	IFIH1	SPLICE-SITE	0.64	2.08
11	18497187	rs145833201	LDHAL6A	SPLICE-SITE	0.09	0.83
17	79974815	rs143008575	ASPSCR1	SPLICE-SITE	0.09	0.83
X	7889837	NA	PNPLA4	STOP-GAINED	<0.01	0.83
X	127185638	NA	ACTRT1	FRAME-SHIFT	0.18	2.08

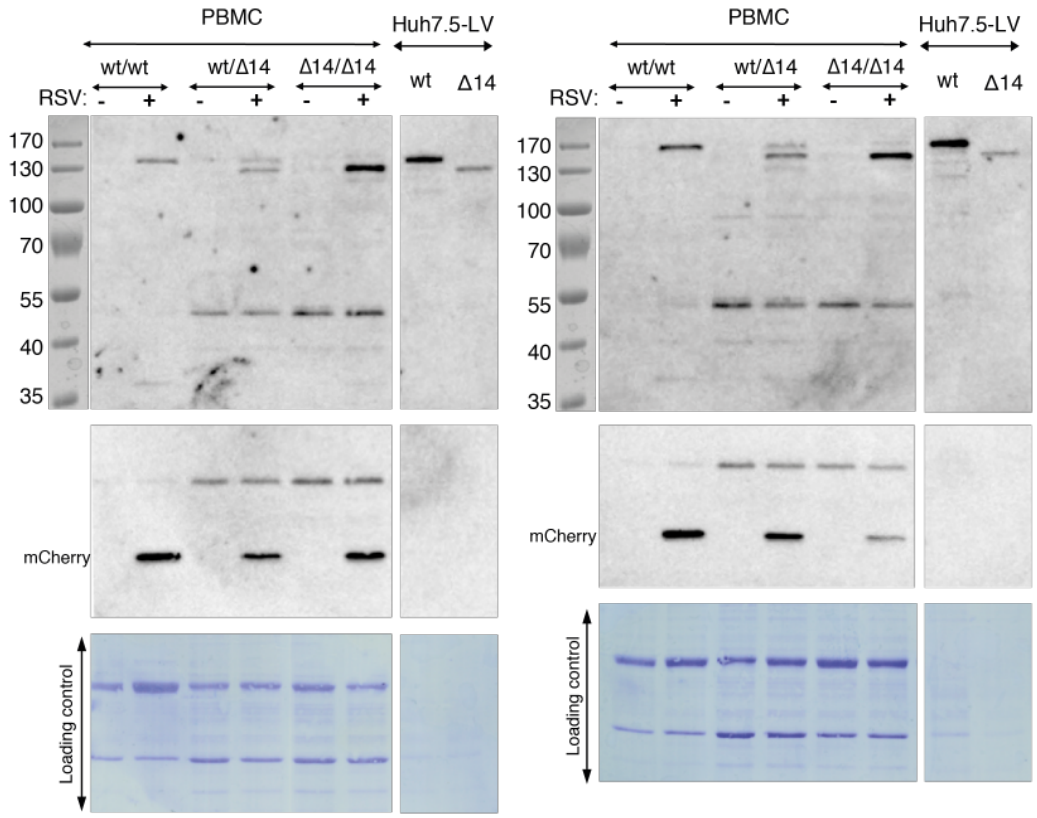

Figure S1. Expression of IFIH1-wt and IFIH1-Δ14 in patients' peripheral blood mononuclear cells. Related to Figure 1.

Expression of IFIH1-wt and IFIH1-Δ14 in peripheral blood mononuclear cells (PBMCs) from an individual homozygous for rs35732034 major allele, from the patient homozygous for rs35732034, and from her heterozygous mother (left) and her heterozygous father (right), as shown by western blot gel with or without RSV infection *in vitro*. Protein expression of both IFIH-wt and IFIH1-Δ14 is boosted by RSV infection, but the increase is particularly dramatic for IFIH1-Δ14. Huh7.5 cells transduced with a lentiviral vector expressing either IFIH1-wt or IFIH1- Δ14 were used as positive controls. Under each gel are shown the expression of mCherry (control for RSV infection) and the

coomassie blue staining (loading control). Molecular weight markers are shown on the left of each gel (kDa).

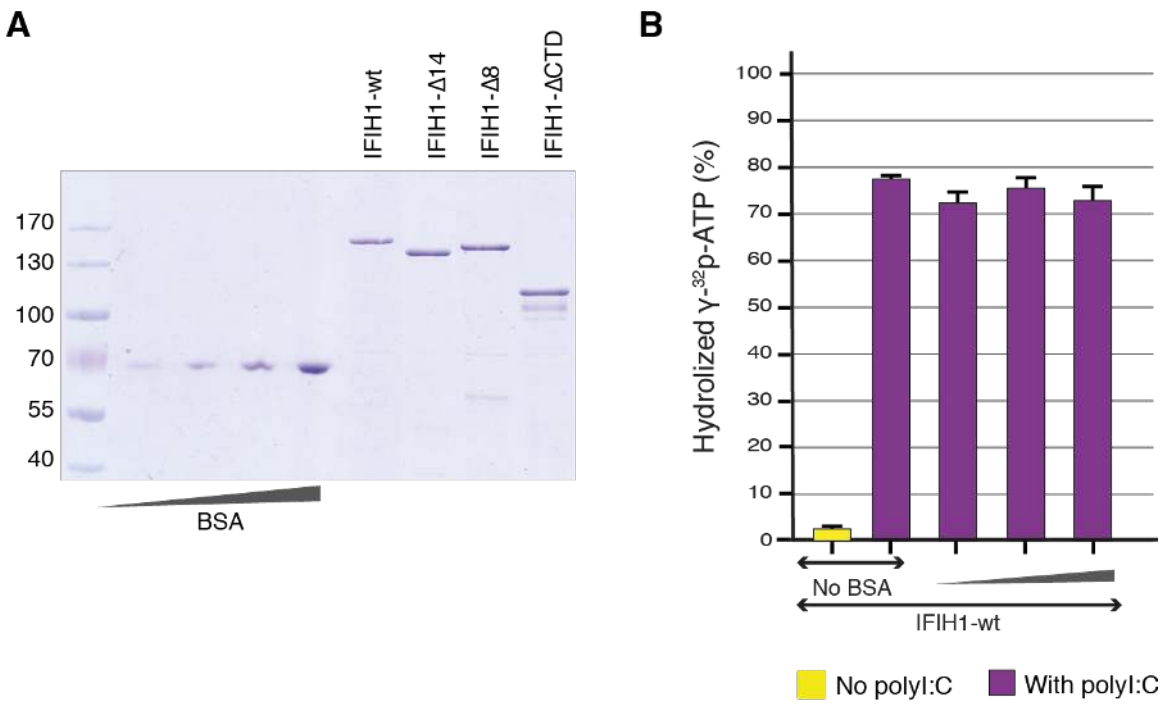

Figure S2. Purification of IFIH1 wild type and mutant proteins. Related to Figure 2. (A) Purified recombinant IFIH1-wt, IFIH1-Δ14, IFIH1-Δ8 and IFIH1-ΔCTD; BSA quantity; 0.1, 0.2, 0.4 and 0.8 µg; (B) BSA does not interfere with ATPase activity of wt protein (300ng wt protein, 150, 300ng or 450ng of BSA, 10ng polyI:C, n=2). Data are represented as mean + SD. BSA, Bovine serum albumin; wt, wild type; polyI:C, polyinosinic:polycytidylic acid.

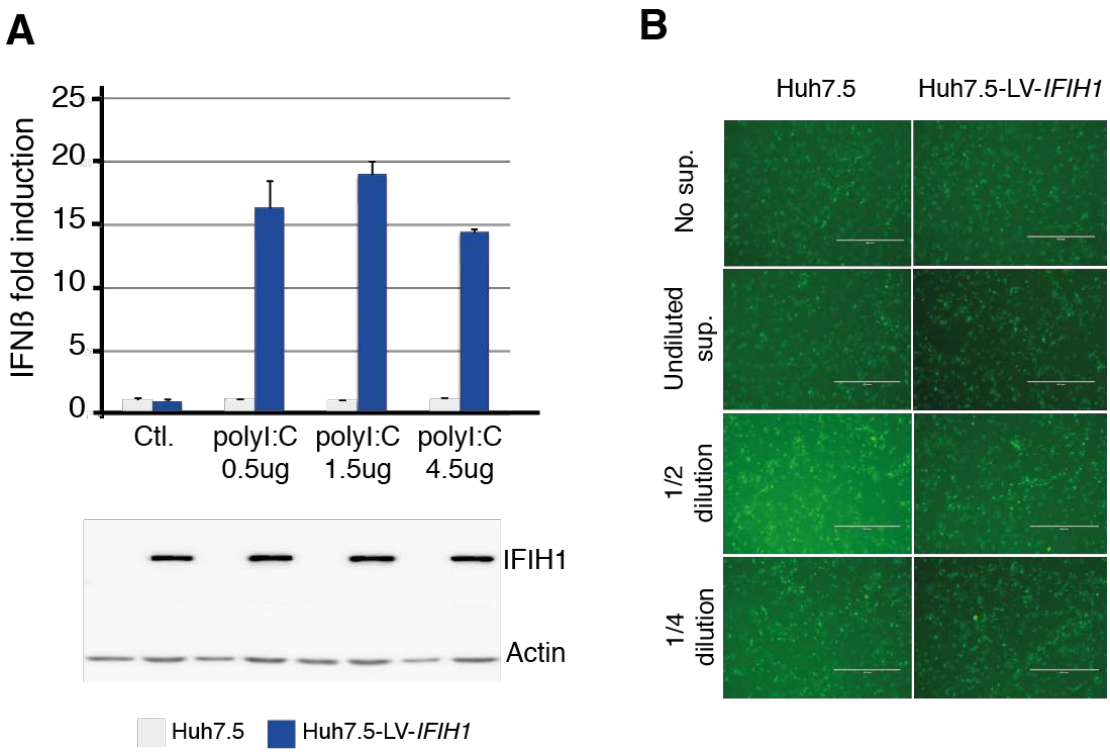

Figure S3. IFIH1 transduction induces IFNβ only in the presence of viral pathogen.

Related to Figure 3.

(A) Huh7.5 cells lack endogenous IFIH1 and do not show any IFNβ induction upon polyI:C stimulation (gray). The cells gain the ability to induce IFNβ after transduction of IFIH1-wt using a lentiviral vector, Huh7.5-LV-*IFIH1* (blue), (n=2); (B) The supernatants of native and IFIH1 transduced Huh7.5 cells were collected and placed on A549 cells for 14 hours; A549 cells were then infected by GFP-tagged vesicular stomatitis virus (VSV-GFP), a rhabdovirus highly sensitive to the antiviral state induced by type 1 interferon. No difference was observed between the two groups, or with the control group (A549 cells without added supernatant) regardless of the supernatant dilution, demonstrating that IFIH1 transduction of huh7.5 cells does not lead to IFNβ induction or to the

establishment of an anti-viral state in the absence of viral stimulation. Data are represented as mean + SD. sup., supernatant.

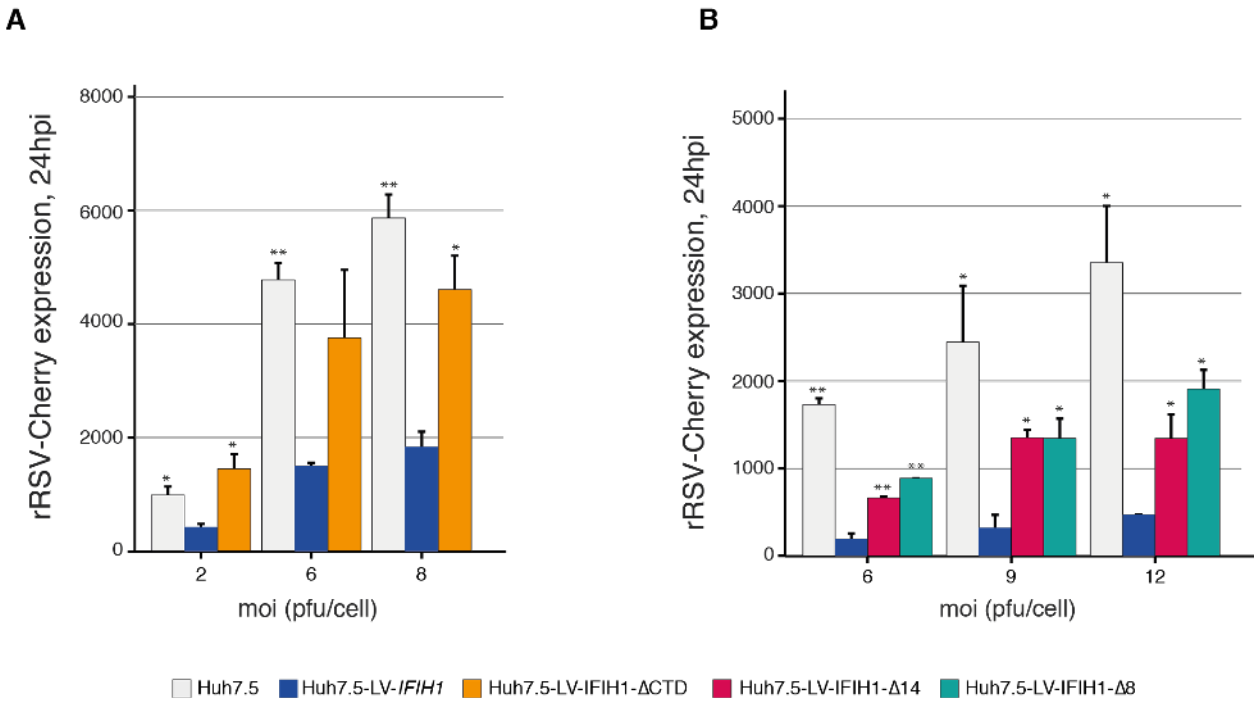

Figure S4. IFIH1 mutant proteins does not reduce RSV replication. Related to Figure 3.

FACS analyses of cherry expressing recombinant RSV in Huh7.5 cells and Huh7.5 cells transduced with a lentiviral vector expressing IFIH1 (Huh7.5-LV-*IFIH*), and compared to (A) Huh7.5-LV-*IFIH1*-ΔCTD transduced cells and (B) Huh7.5-LV-*IFIH1*-Δ14 and Huh7.5-LV-*IFIH1*-Δ8 transduced cells. IFIH1-wt significantly reduced RSV replication at 24 hpi, when compared to either wild type Huh7.5 cells (lacking IFIH1) or Huh7.5 cells transduced with the three mutant vectors, (n=2); *$p<0.05$, **$p<0.01$. Data are represented as mean + SD. moi, multiplicity of infection; pfu, plaque-forming unit; hpi, hours post infection.

Supplementary Materials and Methods

Subject recruitment and specimen collection

Between December 2010 and October 2013, we prospectively enrolled previously healthy children suffering from severe lower respiratory tract infection and requiring invasive or non-invasive respiratory support in five specialized Pediatric Intensive Care Units (PICU) from Australia and Switzerland. The study was approved by the respective institutional Human Research Ethics Committees. Written informed consent was obtained from parents or legal guardians.

Children less than 4 years of age that were admitted to PICU due to a severe respiratory infection of proven or presumed viral origin and required respiratory support were eligible. Exclusion criteria were the presence of any significant underlying disease or comorbidity, including prematurity, congenital cardiac disease, chronic lung disease, sickle cell disease, hepatic, renal, or neurologic chronic conditions, solid and hematological malignancies and known primary immunodeficiency. Respiratory support was defined as non-invasive ventilation including high-flow nasal cannulae (HFNC) and continuous or bilevel positive airway pressure (CPAP and BiPAP), or invasive ventilation including conventional and high frequency oscillation ventilation (HFOV).

The following demographic and clinical information was collected: age, gender, weight, ethnicity, type of ventilation, length of ventilation in days, clinical outcome, microbiological diagnostic procedures and results including rapid antigenic test for RSV and influenza, respiratory virus PCR panel, and viral cultures. For each study participant, we obtained a nasopharyngeal aspirate or endotracheal tube aspirate, 1ml EDTA blood in

vacutainer tubes and 2.5ml blood in PAXgene blood RNA tubes. Samples were immediately frozen at -70 degrees Celsius until shipment, and then analyzed in batch.

Screening of respiratory viruses

Viral RNA was extracted from 100ul of nasopharyngeal aspirate using the NucliSens Easymag© (bioMérieux). Respiratory viruses screening was performed using FTD Respiratory pathogens 21 assay (Fast-track Diagnostics) on a Viia7 instrument (Applied biosystems).

Exome sequencing and alignment

Genomic DNA was extracted from whole blood (QIAGEN, 51104). Exome sequencing libraries were prepared with 2 µg to 3 µg of genomic DNA using Agilent SureSelect reagents (Agilent Technologies, 5190-4627, 5190-4631, 5190-6208 and G9611A). Cluster generation was performed using the Illumina TruSeq PE Cluster Kit v3 reagents. The resulting libraries were sequenced as 100-nucleotide, paired-end reads on Illumina HiSeq 2000 or HiSeq 2500 using TruSeq SBS Kit v3 reagents. Sequencing was done at the Lausanne Genomic Technology Facility. Raw sequencing reads were processed using the Illumina Pipeline Software version 1.82. Purified filtered reads were aligned to human reference genome hg19 using Burrow-Wheeler Aligner version 0.6.2 (BWA) (1). PCR duplicates were removed using Picard (http://picard.sourceforge.net/).

Variant calling and annotation

We used Genome Analysis Toolkit (GATK) (2, 3) version 3.1-1, Platypus (4) version 0.7.9.1 and SAMtools (5) version 0.1.19 to call single nucleotide variants (SNVs) and small insertion and deletions (Indels) from duplicate-marked bam files. With GATK we used HaplotypeCaller for multi-sample variant calling. We followed GATK best practice

to call the variants (https://www.broadinstitute.org/gatk/guide/best-practices?bpm=DNAseq); variants that did not pass GATK filtering were discarded. With Platypus we used callVariants for multi-sample variant calling and variants that did not pass Platypus filtering criteria were discarded. With SAMtools we used mpileup default options for multi-sample variant calling followed by bcftools view to generate the vcf file, variants with quality score below 30 were discarded. Only variants that were present at the intersection of the three variant callers and had a missingness of <5% were kept for downstream analysis.

We used SnpEff (6) version 4.1B to predict the functional impact of variants, and notably to identify putative loss of function variants (LoFs). We defined the following categories of variants as LoFs: stop-gain SNVs, splice site disrupting SNVs, frame-shift indels in the first 95% of the coding region, or deletions removing either the first exon or more than 50% of the coding sequence. We further enriched for LoFs that are more likely to play a functional role by including only LoFs found in genes with a low or medium gene damage index and were affecting all coding transcripts of the gene (7).

RNA sequencing and alignment

Total RNA was extracted from 2.5 ul of whole blood collected in PAXgene tubes using PAXgene blood RNA kit (PreAnalytiX, 762174). Libraries were prepared using the Illumina TruSeq Stranded mRNA (Ribo-Zero Globin) reagents (Illumina, RS-122-2501) using 400ng of total RNA. Cluster generation was performed with the Illumina TruSeq PE Cluster Kit v3 reagents. The resulting stranded libraries were sequenced as 100-nucleotide, paired-end reads on the Illumina HiSeq 2000 using TruSeq SBS Kit v3 reagents. The raw sequencing reads were processed using the Illumina Pipeline Software

version 1.82. Purified filtered reads were aligned to the human reference genome hg19 using STAR (8) version 2.3.0e and the Gencode annotation (9) version 19.

Plasmids

pcDNA3.1(+) containing wild type *IFIH1* was constructed by PCR amplification on pEF-BOS-IFIH1 with sense primer that introduced BamHI site and flag sequence at the N-terminus and with the antisense primer that introduced XhoI site at the C-terminus of IFIH1. The PCR products were digested with BamHI and XhoI and then inserted into pcDNA3.1(+).

pcDNA3.1(+) containing deletion mutant *IFIH1* lacking exon 14 (IFIH1-Δ14) was constructed using a fusion PCR strategy. First, pEF-BOS-IFIH1 was amplified by PCR with sense primer that introduced BamHI site and HA sequence at the N-terminus of IFIH1 and with the antisense primer that inserted the beginning of exon 15 sequence at the end of the exon 13. Second, pEF-BOS-IFIH1 was amplified by PCR with sense primer that introduced the end of exon 13 sequence at the beginning of exon 15 and with the antisense primer that introduced XhoI site at the C-terminus of IFIH1. The resulting PCR products were mixed and amplified by PCR with sense primer that introduced BamHI site and HA sequence at the N-terminus and with the antisense primer that introduced XhoI site at the C-terminus of IFIH1. The PCR products were digested with BamHI and XhoI and then inserted into pcDNA3.1(+).

pcDNA3.1(+) containing deletion mutant *IFIH1* gene lacking exon 8 (IFIH1-Δ8), and pcDNA3.1(+) containing deletion mutant *IFIH1* with stop-gain mutation in exon 10 (IFIH1-ΔCTD), were ordered from life technologies plasmid service. The inserts of the

resulting pcDNA3.1(+) containing IFIH1-wt or mutant plasmids were confirmed by sequencing.

To test IFNβ induction, we used pβ-IFN-fl-lucter containing the firefly luciferase gene driven by the human IFNβ promoter as described previously (10) and pTK-rl-lucter containing the *Renilla* luciferase gene (PROMEGA) driven by the herpes simplex virus TK promoter. pEBS-tom encodes a red fluorescent protein.

Transfection and measure of interferon-β promoter activity

293T cells and Huh7.5 cells were grown in Dulbecco's modified Eagle's medium supplemented with 10% fetal bovine serum and 1% Pen/Strep. 100'000 cells were plated into 6-well plates and transfected 24 hrs later with 1.5 μg of pβ-IFN-fl-lucter, 0.5 μg of pTK-rl-lucter and 0.5 μg of pEBS-tom (used as a transfection control), using Gene Juice transfection reagent (NOVAGEN). Additionally, cells were transfected with 1 μg of IFIH1 encoding plasmids. 24 hrs later, Huh7.5 cells (but not 293T cells) were transfected with elicitor RNA using TransMessenger transfection reagent (QIAGEN) according to the manufacturer's instructions. 20 hrs later, cells were harvested and cell lysates were used to measure firefly and *Renilla* luciferase activity (dual-luciferase reporter assay system, Glomax 20/20 luminometer, PROMEGA).

Protein expression in the cell lysates was then checked by Western blotting, using the following primary antibodies: anti-RIG-I (1:1000) (Alexis ALX-210-932), anti-IFIH1 (1:1000) (Alexis ALX-210-935), anti-HA (1:2000) (Enzo Life Sciences ENZ-ABS-118-0500), anti-flag (1:1000) (Sigma F1804-1MG). Immunoblot analyses were developed with the following secondary antibodies: goat anti-mouse and anti-rabbit IgG horseradish peroxidase conjugated whole antibody (1:3000) (Bio-Rad). ImageJ version 1.44p

(http://imagej.nih.gov/ij/) was used for western blot quantifications.

Viruses

Respiratory syncytial virus expressing Green Fluorescent Protein (RSV-GFP, obtained from Mark Peeples (11)) or mCherry (rRSV-mCherry obtained from Jean-François Eléouët (12)) stocks were amplified in A549 (human alveolar adenocarcinoma cell line) cells. RSV-GFP stocks titers were determined using serial dilutions to infect A549 cells. GFP or mCherry expression was measured by flow cytometry on 20'000 cells (*i.e.* 10% of the harvested cells) using BD Accuri C6 Cytometer. Data were analyzed using CFlow Plus software (Accuri, version 1.0.264.15). Fluorescence pictures were acquired using Evos FL epifluorescence microscope. Recombinant vesicular stomatitis virus expressing Green Fluorescent Protein (rVSV-GFP obtained from Jacques Perrault (13)) stocks were amplified in 293T cells and stocks titers were determined using serial dilutions to infect 293T cells. GFP expression was measured by flow cytometry on 20'000 cells (*i.e.* 10% of the harvested cells) using BD Accuri C6 Cytometer. Data were analyzed using CFlow Plus software (Accuri, version 1.0.264.15). Fluorescence pictures were acquired using Evos FL epifluorescence microscope.

Measure of protein stability by pulse chase

Transfected 293T cells were incubated for 30 minutes at 37°C in methionine-free, cysteine-free and FCS-free DMEM. 100 µCi/ml of 35S-methionine + 35S-cysteine labelling mix (HARTMAN Analytic) was added and cells were incubated at 37°C for 30 minutes. The chase (0, 2, 4, and 8 hours) was performed at 37°C in DMEM supplemented with unlabelled methionine and cysteine (10mM). Cell lysates were loaded on 7.5% acrylamide gels, transferred to a PVDF membrane and exposed to autoradiography.

Results were revealed in a phosphorimager (Typhoon, GE Healthcare Life Sciences) and quantified with ImageQuantTL software (GE Healthcare Life Sciences).

Recombinant IFIH1 expression

IFIH1 inserts cloned into pcDNA3.1(+) were inserted into pET28-His10Smt3 backbone. pET28-His10Smt3-IFIH1 wt or ΔCTD plasmids were transformed into *E. coli* BL21. Cultures (500 ml) derived from single transformants were grown at 37°C in LB medium containing 50 µg/ml kanamycin to an A_{600} of 0.6. The cultures were adjusted to 0.2 mM IPTG and 2% ethanol and further incubated for 20 hours at 17°C. Cells were harvested by centrifugation and recombinant RIG-I protein was purified from bacteria as previously described (14). Protein concentration was determined using the Bio-Rad dye binding method with BSA as the standard.

Measure of IFIH1 ATPase activity

Increasing amounts of polyI:C were incubated with 200 nM of purified recombinant IFIH1, [(Isqb) γ-^{32}P] ATP (Hartmann Analytic) in a final volume of 15 µl (50 mM Tris acetate pH 6, 5 mM DTT, 1.5 mM $MgCl_2$) for 15 minutes at 37°C. Reactions were then stopped with 1 mM formic acid and 2.5 µl of each reaction were spotted onto TLC PEI Cellulose F plates (MERCK 1.05579.0001) and applied to a migration buffer (LiCl 0.5 M and formic acid 1 N) to separate released $^{32}PO_4$ and non hydrolyzed ATP. $^{32}PO_4$ release was measured in a phosphorimager (Typhoon, GE Healthcare Life Sciences) and quantified with ImageQuantTL software (GE Healthcare Life Sciences). ATPase data were processed as follow: for each sample, the ratio free $^{32}PO_4$/non hydrolyzed ATP was calculated (and reported to the final ATP concentration in the reaction); fold increases were obtained by normalizing the calculated ATPase activity to the ATPase activity of

the protein alone (control without RNA).

Cell culture and transduction with lentiviral vectors

The 293T cells lines were cultured in Dulbecco's modified Eagle's medium supplemented with 10% fetal calf serum. All recombinant lentiviruses were produced by transient transfection of 293T cells according to the following protocol. 5 x 10^6 293 cells were plated in 10 cm PD and cotransfected with 15 µg of a plasmid vector (pLV.CMV.IFIH1.IRES-GFP and pLV-U6-empty-PGK-GFP), 10 µg of psPAX2 and 5 µg of pMD2G-VSVG by calcium phosphate precipitation. After 8 hours, medium was changed and recombinant lentiviruses vectors were harvested 24 hours later. Huh7.5 cell lines, platted in 6-well plates, were transduced at an MOI of 2 with the recombinant lentiviruses. Two days after transduction, GFP-expressing cells were sorted by FACS.

Quantitative RT-PCR

Total RNA isolation was performed by using the NucleoSpin RNA kit (Macherey-Nagel) according to the manufacturer's instruction. 200 µg of total RNA from infected cells pellet was used for cDNA synthesis using the Omniscript RT Kit (QIAGEN). Quantitative RT-PCR was performed by using 2 µL of cDNA and 18 µL of Taqman Fast universal PCR master mix (Thermo Fisher Scientific) containing specific primers (20 µM) and probes (5 µM) for human rhinovirus (HRV). 7500 fast Real-Time PCR System (Thermo Fisher Scientific) was used to perform PCR reactions. The ΔΔCT method was used to quantify the mRNA expression levels of endogenous genes. The mRNA expression levels of endogenous genes were normalised to the housekeeping gene 18S rRNA. Viral RNA copy numbers were obtained through the generation of a standard curve obtained with serial dilutions of a plasmid containing HRV cDNA.

Statistical analysis

Independent two-tailed t-tests for all functional tests were performed using R (version 1.65).

Purification of peripheral blood mononuclear cells

Human PBMCs were extracted from heparinised blood using a standard density gradient centrifugation over Ficoll-Paque PLUS (GE Healthcare, Uppsala, Sweden). Cell viability was enumerated by 0.4% Trypan blue (Gibco, Mulgrave, VIC) exclusion. 10^7 cells were stored until required in liquid nitrogen vapour phase in 1mL freezing media consisting of heat-inactivated FCS (Gibco, Mulgrave, VIC) with 10% DMSO (Sigma, D8418).

Supplementary References

1. Li H, Durbin R (2009) Fast and accurate short read alignment with Burrows-Wheeler transform. *Bioinformatics* 25:1754–60.
2. McKenna A et al. (2010) The Genome Analysis Toolkit: a MapReduce framework for analyzing next-generation DNA sequencing data. *Genome research* 20:1297–303.
3. Van der Auwera GA et al. (2013) From FastQ data to high confidence variant calls: the Genome Analysis Toolkit best practices pipeline. *Curr Protoc Bioinformatics* 43:11.10.1–33.
4. Rimmer A et al. (2014) Integrating mapping-, assembly- and haplotype-based approaches for calling variants in clinical sequencing applications. *Nature genetics* 46:912–8.
5. Li H et al. (2009) The Sequence Alignment/Map format and SAMtools. *Bioinformatics* 25:2078–9.
6. Cingolani P et al. (2012) A program for annotating and predicting the effects of single nucleotide polymorphisms, SnpEff: SNPs in the genome of Drosophila melanogaster strain w1118; iso-2; iso-3. *Fly* 6:80–92.
7. Itan Y et al. (2015) The human gene damage index as a gene-level approach to prioritizing exome variants. *Proc Natl Acad Sci USA* 112:13615–20.
8. Dobin A et al. (2013) STAR: ultrafast universal RNA-seq aligner. *Bioinformatics* 29:15–21.
9. Harrow J et al. (2012) GENCODE: the reference human genome annotation for The ENCODE Project. *Genome Res* 22:1760–74.
10. King, Goodbourn (1994) The beta-interferon promoter responds to priming through multiple independent regulatory elements. *The Journal of biological chemistry* 269:30609–15.
11. Hallak LK, Collins PL, Knudson W, Peeples ME (2000) Iduronic acid-containing glycosaminoglycans on target cells are required for efficient respiratory syncytial virus infection. *Virology* 271:264–75.
12. Rameix-Welti M-AA et al. (2014) Visualizing the replication of respiratory syncytial virus in cells and in living mice. *Nat Commun* 5:5104.
13. Ostertag D, Hoblitzell-Ostertag TM, Perrault J (2007) Overproduction of double-stranded RNA in vesicular stomatitis virus-infected cells activates a constitutive cell-type-specific antiviral response. *J Virol* 81:503–13.
14. Hausmann S, Marq J-BB, Tapparel C, Kolakofsky D, Garcin D (2008) RIG-I and dsRNA-induced IFNbeta activation. *PLoS ONE* 3:e3965.